NREL/TP-473-7783 • UC Category: 1505 • DE95009207

Thermal Management of Batteries Using a Variable-Conductance Insulation (VCI) Enclosure

Steven D. Burch
Richard C. Parish
Matthew A. Keyser
National Renewable Energy Laboratory

Prepared for the Intersociety Energy Conversion Engineering Conference, Orlando, Florida, July 31-August 4, 1995

National Renewable Energy Laboratory
1617 Cole Boulevard
Golden, Colorado 80401-3393
A national laboratory of the U.S. Department of Energy
Managed by the Midwest Research Institute
for the U.S. Department of Energy
under Contract No. DE-AC36-83CH10093

May 1995

NOTICE

Available to DOE and DOE contractors from:
Office of Scientific and Technical Information (OSTI)
P.O. Box 62
Oak Ridge, TN 37831
Prices available by calling (615) 576-8401

Available to the public from:
National Technical Information Service (NTIS)
U.S. Department of Commerce
5285 Port Royal Road
Springfield, VA 22161
(703) 487-4650


Printed on paper containing at least 50% wastepaper and 10% postconsumer waste

THERMAL MANAGEMENT OF BATTERIES USING A VARIABLE-CONDUCTANCE INSULATION (VCI) ENCLOSURE

Steven D. Burch, Richard C. Parish, and Matthew A. Keyser

National Renewable Energy Laboratory
1617 Cole Boulevard, MS 27/2
Golden, Colorado 80401-3393
(303) 384-7480 (FAX: -7411)

ABSTRACT

Proper thermal management is important for optimum performance and durability of most electric-vehicle batteries. For high-temperature cells such as sodium/sulphur, a very efficient and responsive thermal control system is essential. Heat must be removed during exothermic periods and retained when the batteries are not in use. Current thermal management approaches rely on passive insulation enclosures with active cooling loops that penetrate the enclosure. This paper presents the design, analysis, and testing of an enclosure with variable conductance insulation (VCI). VCI uses a hydride with an integral electric resistance heater to expel and retrieve a small amount of hydrogen gas into a vacuum space. By controlling the amount of hydrogen gas, the thermal conductance can be varied by more than 100:1, enabling the cooling loop (cold plate) to be mounted on the enclosure exterior. By not penetrating the battery enclosure, the cooling system is simpler and more reliable. Also, heat can be retained more effectively when desired. For high temperatures, radiation shields within the vacuum space are required. Ceramic spacers are used to maintain separation of the steel enclosure materials against atmospheric loading. Ceramic-to-ceramic thermal contact resistance within the spacer assembly minimizes thermal conductance.

Two full-scale (0.8-m × 0.9-m × 0.3-m) prototypes were designed, built, and tested under high-temperature (200°–350°C) battery conditions. With an internal temperature of 330°C (and 20°C ambient), the measured total-enclosure minimum heat loss was 80 watts (excluding wire pass-through losses). The maximum heat rejection was 4100 watts. The insulation can be switched from minimum to maximum conductance (hydrogen pressure from 2.0×10^{-3} to 8 torr) in 3 minutes. Switching from maximum to minimum conductance was longer (16 minutes), but still satisfactory because of the large thermal mass of the battery.

INTRODUCTION

Increasing concerns in the United States and worldwide about urban air pollution and dependence on imported oil have led to a variety of new regulations. In a bold move, California enacted regulations requiring 2% of all vehicles sold in that state in 1998 to be zero-emission vehicles (ZEVs), meaning zero tailpipe emissions. Furthermore, the legislation requires the sale of 5% ZEVs in 2001 and 10% ZEVs in 2010. Similar regulations have been enacted, or are being considered, by state legislatures in other areas of the United States. With the current state of technology, zero tailpipe emissions are attained only by electric vehicles.

Recognizing that state-of-the-art battery capability was an impediment to meeting the governmental legislation, the Chrysler Corporation, Ford Motor Company, and General Motors Corporation formed the U.S. Advanced Battery Consortium (USABC) in January 1991, as a collaborative research and development venture to identify and develop the most promising advanced battery technologies for future electric vehicles. The 4-year, $260 million program is 50% funded by the U.S. Department of Energy (DOE), with the Electric Power Research Institute (EPRI) providing support on behalf of electric utilities.

The goals of the USABC are to develop battery technologies which meet mid-term performance criteria of 150–200 W/kg specific power, 80–100 W·h/kg specific energy, a 5-year life, and a cost of $150/kW·h or less. Long-term battery goals push specific power to 400 W/kg and specific energy to 200 W·h/kg, with a 10-year life, costing less than $100/kW·h.

To make use of expertise in the DOE national laboratories, the USABC participates in cooperative research and development agreements (CRADAs) with selected laboratories. The USABC signed an agreement with the National Renewable Energy Laboratory (NREL) in June 1992 to develop thermal control techniques for high-temperature batteries. The 32-month project culminated in the successful demonstration of a full-scale test

enclosure which met the thermal performance criteria established by the USABC.

The intended batteries (sodium/sulphur) must be maintained in the temperature range of 320–350°C without imposing unsafe or uncomfortable conditions on the occupants. During normal operation and during rapid recharge, heat rejection from the battery pack is required due to internal resistance heating. However, heat retention is necessary during quiescent periods and slow recharges to prevent stored energy from being lost.

Methods previously used to provide thermal control for high-temperature batteries include the circulation of a working fluid within the battery enclosure, absorbing the excess heat from heat exchangers in contact with the battery cells (Nowbilski and Acharya; 1985, Lee et al., 1984). This method has proved somewhat inadequate due to difficulties associated with excessive heat loss during battery quiescent periods and potential leakage of the elevated-temperature fluid.

An alternate concept for thermal management of the battery pack is to design an enclosure whose thermal conductance is variable and controllable. Researchers at NREL have developed concepts for responsive insulating materials that are very compact and durable and in which the heat flow can be modulated to match the time-varying needs of the application. This insulation concept has been identified as variable-conductance insulation or VCI (Benson et al., 1994). VCI has been applied to a variety of applications including thermal management of automotive catalytic converters (Burch et al., 1995). In its "normal" insulating state, the VCI demonstrates a very low thermal conductance. When triggered, the VCI's thermal conductance increases to a large value, allowing for large heat flow through the insulation. The level of heat flow can be regulated by selecting intermediate levels of the control. By eliminating pass-throughs for internal air or liquid cooling systems, the variable-conductance enclosure concept greatly reduces thermal control system complexity and associated quiescent heat losses.

VCI uses multi-layer vacuum insulation with a controllable hydrogen source. The hydrogen source is a metal hydride that absorbs or desorbs hydrogen as a function of its temperature. This characteristic is used to vary the pressure of hydrogen gas within the vacuum insulation. At room temperature, the hydride absorbs and retains hydrogen and other residual gases, maintaining a low vacuum pressure within the insulation. At elevated temperatures, the hydride desorbs hydrogen, causing the pressure within the insulation to rise. The conductance of the insulation increases with increasing pressure of the hydrogen. The hydrogen gas, therefore, acts as a controllable thermal conductor within the evacuated insulation, changing the heat conduction characteristics as a function of its pressure.

The vacuum insulation consists of a double-walled metal envelope whose internal volume has been evacuated. This removes the gas-phase thermal conductance, leaving only radiation and solid-phase conduction. The envelope sides are separated against the force of external atmospheric pressure by either inherent structural rigidity (as in the cylindrical "Thermos" bottle or Dewar flask) or by the inclusion of an internal, low-thermal-conductivity structural material, such as a powder, compressed multi-layer insulation, or discrete supports. The inherent structural instability of a rectilinear geometry, as proposed for most electric vehicle battery-pack enclosures, dictates the use of an internal method to maintain envelope separation. However, for use as a variable-conductance insulation, a minimum of internal complexity is necessary to allow for the free flow of the thermally conductive hydrogen gas. This results in a vacuum insulation that contains an adequate number of glass paper and aluminum foil layers to limit radiation heat transfer for the high-temperature battery application, but that also contains low-thermal-conductivity "spacer" stacks to maintain the separation of the metal envelope facesheets while limiting the solid-phase conduction. This basic geometry was the preliminary concept of variable-conductance vacuum insulation.

FULL-SCALE TEST ARTICLE (FSTA) DESIGN

As a means of demonstrating the VCI technology in a representative configuration, two full-scale test articles for high-temperature battery thermal management were designed, built, and tested. The first test article (FSTA1) was empty, whereas the second test article (FSTA2) contained a battery simulator of representative size and mass. The objectives were to:

1. Design a box-within-a-box VCI enclosure from experience and analysis (including 3-D finite element thermal and structural analysis) that could meet the performance and durability goals.

2. Assess the stability of ceramic spacer stacks exposed to structural and thermal stresses.

3. Determine the reaction of 0.51-mm (20-mil) inner membrane to thermal and vacuum stresses.

4. Evaluate minimum heat loss (goal: $\leq$ 100 W at 300°C)

5. Evaluate maximum heat removal (goal: $\geq$ 4000 W at 315°C).

6. Assess the metal hydride effectiveness.

The design of FSTA1 and FSTA2 is very similar and is shown in Figures 1 and 2. The design uses a "box within a box" approach in which the battery core is sealed within an inner box surrounded by multi-layer insulation. This assembly is enclosed by an outer box. Water/glycol heat exchangers are incorporated on the top and bottom surfaces of the outer box to remove heat during the maximum-conductance mode of the insulation. This approach was chosen because of the inherently low thermal loss for this type of construction. Further design elements include:

Battery Simulator In FSTA2, thick aluminum slabs were stacked vertically, with electric resistance sheet heaters sandwiched between them, to serve as a battery simulator. This block had a total mass of 370 kg. To enhance radiant heat transfer from the block to the top and bottom VCI, the block (and inner VCI) surfaces were coated with boron nitride (emissivity = 0.8). To further direct heat from the block to the cold plates at the top and bottom of the enclosure, 25 mm of porous ceramic insulation were used around the sides of the block (between the block and the inside surface of the VCI).

Inner and Outer Shells The inner shell is composed of 17-7 precipitation-hardened stainless-steel sheets 0.51 mm (0.020") thick. It is made by laser-welding four individual pieces for the sides and one for the bottom, while the top piece is clamped in place. The stainless-steel bellows feedthrough is welded to the top piece of the inner box. The top piece is then welded into place after the battery has been incorporated into the inner box.

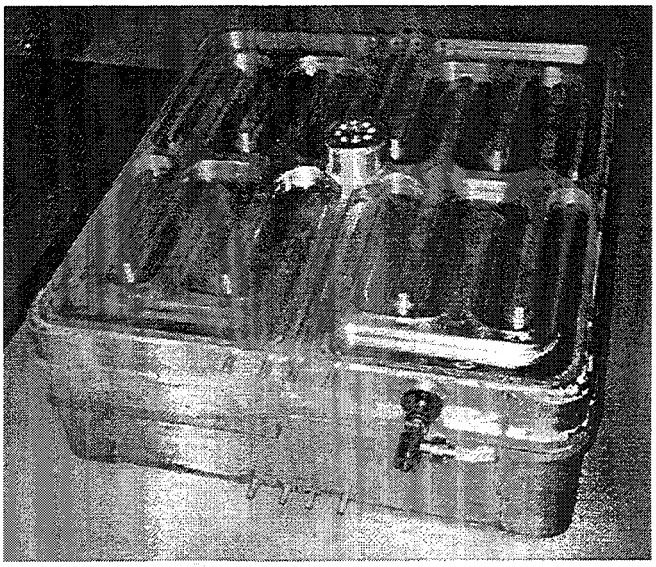

FIGURE 1 - PHOTO OF SECOND FULL-SCALE TEST ARTICLE (FSTA2); COLD-PLATE IS EXPOSED

The outer shell is a series of component parts integrally assembled to incorporate the inner box and the multi-layer insulation blankets, which include the ceramic spacer stacks. The top and bottom heat-exchanger plates are machined from 6061 aluminum plate. The inner side plates are bent aluminum sheet welded onto both top and bottom plates. The bellows is attached to the top plate of the outer shell using a bimetallic, gasketed flange to join the dissimilar metals. The top and bottom surfaces of the outer shell are aluminum sheets mechanically fastened over the heat-exchanger flow channels.

Radiation Shields There are twenty 0.025-mm-thick aluminum shields separated by 20 sheets of 0.20-mm (0.008") glass (silica) paper to minimize thermal shorting due to interlayer contact. Because of the holes for the spacers, the sheets and the foils did not need to be perforated to allow movement of the molecular hydrogen throughout the vacuum cavity. However, to prevent thermal radiation interchange through the spacer holes, three aluminum washers which fit more tightly around the spacer stack were incorporated into the layup. This feature of the blanket design added greatly to fabrication time. Future designs will allow a more snug fit of the blankets to the spacer stack.

Ceramic Spacers The spacers provide the structural support required to maintain the spacing between the inner and outer shells under vacuum. Because these standoffs directly bridge the inner shell (heat source) to the outer shell (heat sink), their thermal conductivity has a large influence on the overall thermal loss for the enclosure. Ceramic is the material of choice because of its high hardness (small contact areas under pressure), high strength, and low thermal conductivity.

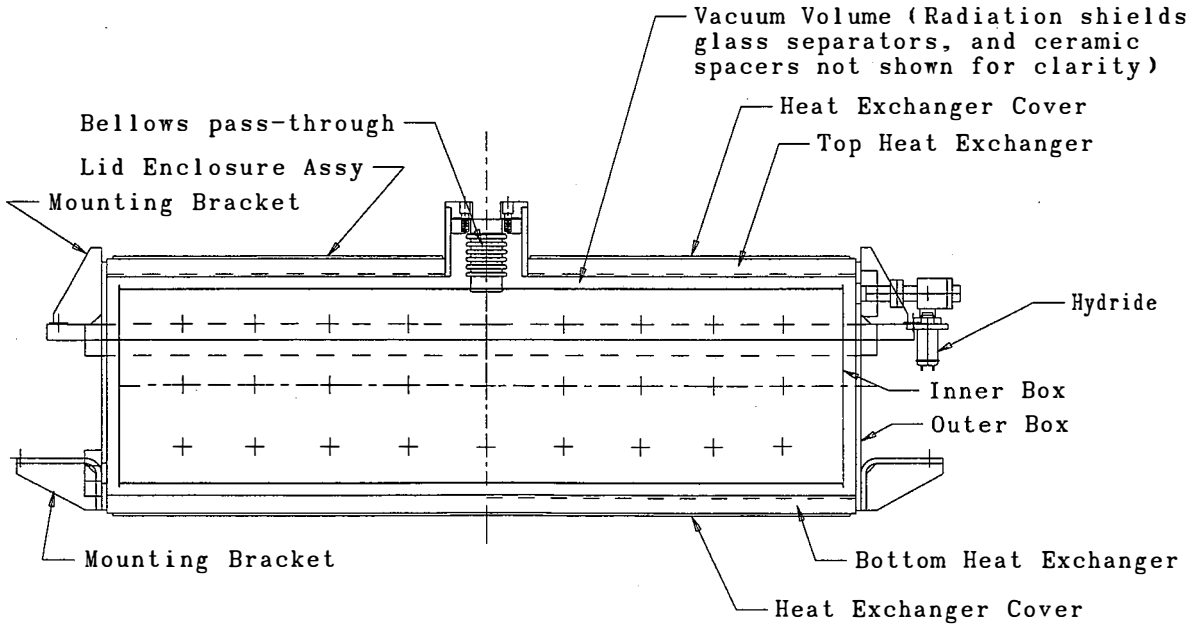

FIGURE 2 - SIDE-VIEW DRAWING OF FSTA2

To adequately support the inner box under vacuum and thermal expansion conditions, 246 zirconia spacer stacks are used, providing a square-pattern spacing of about 100 mm and a stack height of 15 mm. FSTA1 uses 5-piece "four-leg" spacers on a metal rivet pivot point and a metal top cap. Each spacer makes four ceramic-to-ceramic contacts with the adjoining spacer. To reduce conduction heat flow through the spacers, FSTA2 uses a stack of eight "three-leg" spacers with three smaller ceramic-to-ceramic point contacts. To reduce radiant heat loss in this region, the spacers were coated with aluminum. Aluminum washers were inserted in the stackup to block the spacer-to-shield gap.

Penetration Bellows The purpose of the bellows is to provide a vacuum closeout that will allow electrical wires to pass through to the inside of the enclosure (power leads, in the case of an actual battery). One flange is welded to the inside shell and the other is welded to the outside shell. Aluminum/stainless-steel bimetal material was used at the outer flange to enable proper welding. The bellows is made of stainless steel and is 0.51 mm (0.020") thick in the flexible portion.

Reversible Hydrogen Source (Hydride) The hydride consists of a resistively heated, porous metal canister containing metal hydride powder. The hydride is mounted to a vacuum flange electrical feedthrough. A thermocouple is typically attached to the outer surface of the canister. The hydride/thermocouple flange assembly is bolted to the outer shell of the FSTA using a metal gasket.

THERMAL AND STRUCTURAL TEST RESULTS

FSTA1 and FSTA2 were subjected to a variety of thermal tests to determine their performance compared to predictions and to the established USABC requirements. In addition, verification of the design to withstand the structural loads induced by the external atmospheric pressure and thermal stresses was necessary.

Structural Integrity

The ceramic (zirconia) spacer stacks were very stable, under both pressure and thermal loading. No tipping of the stacks was identified during thermal testing, but it should be noted that no shock or vibration testing was performed. Some "popping" sounds were noticed during rapid thermal transients, when hydrogen was injected or withdrawn; however, it is unclear at this point whether this sound is caused by the stacks shifting due to thermal expansion, or cracking of the top spacer as was observed in earlier spacer loading tests. A thicker zirconia spacer or steel top cap may be needed in this design to assure long-term durability.

The deformation of the 0.51-mm-thick inner (hotside) VCI membrane was well behaved, showing no signs of wrinkling or failure. A plaster cast of the FSTA1 inner box was made prior to disassembly. A maximum deformation of 2.4 mm was measured between spacers near the outer edge of the membrane. Finite-element modeling had predicted a maximum value of 2.5 mm.

Minimum Heat Loss

Both FSTA1 and FSTA2 were tested for minimum heat loss (with $P_{H2} < 1\times10^{-3}$ torr). Because FSTA1 was empty (no battery simulator), an electric resistance cartridge heater was inserted through the 38-mm-diameter bellows and used to radiantly heat the inner box. The steady-state heat loss of the enclosure was calculated from the total electric power input to the heater, $Q_T=VI$, with a small (<10%) correction for heat loss from the heater and internal thermocouple leads. Figure 3 shows the corrected enclosure heat loss versus inner box temperature. The loss at 300°C was 132 W, 32% in excess of the goal of 100 W. Primary sources of experimental uncertainty in this heat-loss measurement are the current reading (±4%), the correction for electrical lead losses (±2%), and the system thermal stability (±3%). The total experimental uncertainty (95% confidence) is estimated to be ±6%.

As noted earlier, the primary differences between FSTA1 and FSTA2 are the ceramic spacer stacks and the use of a battery

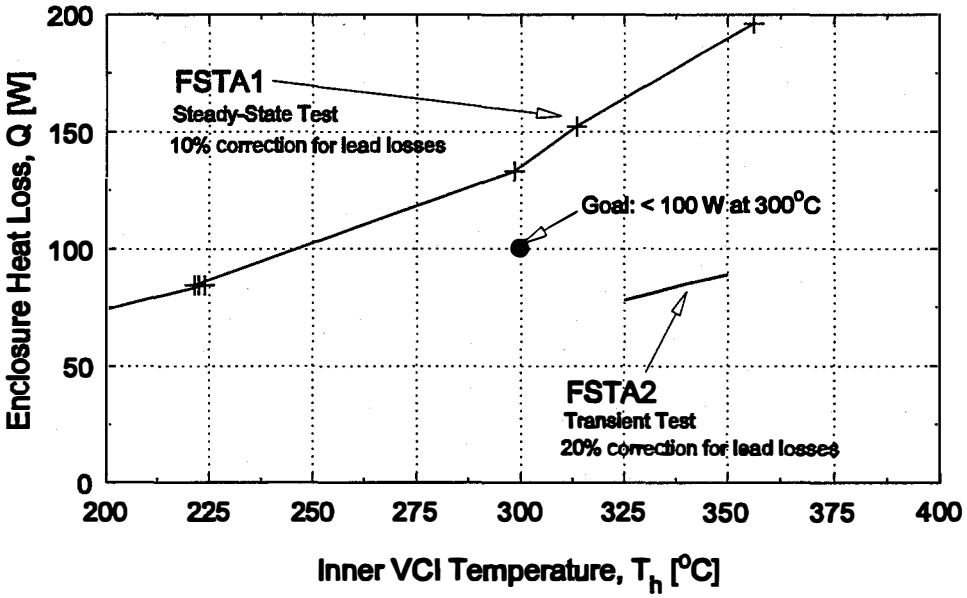

FIGURE 3 - FSTA1 AND FSTA2 MINIMUM HEAT LOSS VERSUS INNER VCI TEMPERATURE

simulator in FSTA2. FSTA2 used a spacer stack with greater thermal resistance (8 versus 5 spacers/stack, 3 versus 4 contact points/spacer). The spacers in FSTA2 were also aluminum-coated for minimum radiative heat loss. The battery simulator used in FSTA2 was made from 370 kg of aluminum. This large thermal mass made it difficult to obtain truly steady-state conditions in a timely manner. Two attempts yielded a minimum heat loss between 60 and 80 W at 300°C.

A transient heat-loss approach was then used for FSTA2. By heating the battery simulator to 350°C, then cutting all electric power to the heaters, the heat loss versus battery simulator (block) temperature could be calculated from the drop in block temperature with time and the thermal capacitance of the block:

$$Q_T = m\, c_p\, (dT/dt)$$

Due to the sizing of the heaters, the correction for heat loss through the leads was greater for FSTA2 (approximately 20%). Figure 3 shows corrected heat loss versus block temperature. The goal of $\leq$ 100 W is met for all block temperatures < 360°C. Extrapolating the corrected data to 300°C, the enclosure heat loss would be 65 W, 35% better than the goal. The primary sources of experimental uncertainty for the transient heat-loss test are the correction for electrical lead losses (±5%), the battery simulator temperature (±3%) and heat capacity (±5%). The mass of the battery simulator was well-known (±1%), as was its composition (99% aluminum). The overall experimental uncertainty of the transient minimum heat-loss data was ±8%.

By dividing the minimum heat loss by the total enclosure interior surface area (2.16 m^2) and the interior-to-exterior temperature difference, an effective VCI minimum thermal conductance can be calculated. For example, at 330°C (20°C ambient), the FSTA2 heat loss was 80 W, hence the thermal conductance was 0.12 W/m^2K. So in its minimum conduction mode, the thermal insulation behavior of the 15 mm-thick VCI is equivalent to about 330 mm of non-vacuum fibrous ceramic insulation.

Maximum Heat Removal

FSTA2 was also tested for maximum heat-rejection capability. Based on prior conductance-versus-hydrogen pressure tests, a hydrogen pressure of 20 torr (0.026 bar) was selected to meet the maximum heat-rejection goal of 4000 W at 315°C block temperature. The steady-state heat-loss approach was used, due to the higher heat-loss rate. Figure 4 shows the FSTA2 heat loss and thermal conductance. Also shown are the hydrogen pressure and the heat removed by the top and bottom FSTA2 cold plates.

From this figure, it is seen that at a steady-state block temperature of 334°C and a pressure of 19 torr, the enclosure heat removal rate was 4100 W. Of the total, 2000 W were extracted by the bottom cold plate and 1800 W by the top cold plate. The remaining 300 W is estimated for the convective heat loss from the enclosure sides. The top-to-bottom difference (1800 versus 2000 W) compares well with predictions, based on the top and bottom differences in the thermal contact resistance from the block to the cold plate.

Other observations include an expected drop in inner VCI temperature at the bellows (due to greater heat loss) and on the sides (due to 25 mm of ceramic insulation between the sides of the block and the VCI).

Primary sources of experimental uncertainty in this maximum-heat-loss measurement are the current reading (±4%) and the system thermal stability (±5%). The total experimental uncertainty is estimated to be ±8%. Because the majority of the heat in the maximum-heat-loss case exits the enclosure at the top and bottom, the VCI maximum thermal conductance is calculated based on the area, heat loss, and temperature difference at the top or bottom, instead of the entire enclosure. For example, at the bottom, the cold plate removed 2000 W of heat through an area of 0.50 m^2. The interior VCI temperature was 330°C, and the exterior VCI temperature was 20°C. Hence, the maximum thermal conductance was 13 W/m^2K, equivalent to about 3 mm of fibrous ceramic insulation. Compared to the minimum VCI thermal conductance of 0.12 W/m^2K, this vacuum insulation exhibited a thermal conductance range of greater than 100:1.

The maximum-heat-loss test was repeated with a block temperature of 305°C. A heat loss of 3900 W was measured. Hence, at 315°C, a heat loss very close to the goal of 4,000 W would be expected. To confirm the capability of FSTA2 to reject more heat at a higher hydrogen pressure, a final test was run with 89 torr (0.12 bar) of hydrogen. At a steady-state block temperature of 348°C, a heat loss of 5665 W was measured. At 315°C, the estimated heat loss at this hydrogen pressure would be 5095 W (27% greater than the goal).

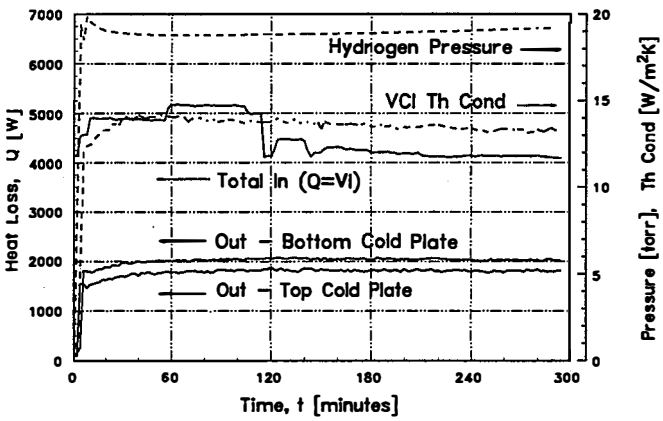

FIGURE 4 - FSTA2 MAXIMUM HEAT LOSS, CONDUCTANCE, PRESSURE

Hydride Effectiveness and Block Temperature Response

Heat loss and thermal conductance were evaluated in FSTA2 at two hydrogen pressures. At 19 torr, the thermal conductance was 13 W/m^2K, and at 89 torr, 22 W/m^2K. These values are in good agreement with data from other small-scale VCI studies at NREL.

A 2.2 g hydride (St707 manufactured by SAES Getters, S.P.A.) charged to 77 torr·l/g was attached to FSTA1 to evaluate the hydrogen expulsion and reabsorption rates. The results are shown in Figure 5. From this figure it can be seen that this single hydride is somewhat undersized, providing a maximum hydrogen pressure of only 8 torr. A larger quantity of hydride would be needed to provide the desired 20 torr. A minimum pressure of 0.0006 torr was achieved, despite a small leak in the inner box welds. This pressure

is sufficiently low to provide the needed minimum thermal conductance.

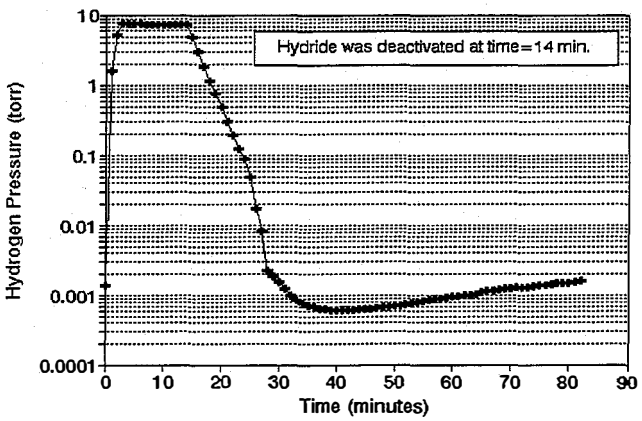

FIGURE 5 - FSTA1 HYDROGEN PRESSURE VERSUS TIME

The hydrogen expulsion rate is fast, reaching the maximum value in under 3 minutes. Hydrogen reabsorption is slower, requiring approximately 16 minutes to drop from 8 to 0.001 torr. Using the conductance-versus-pressure data from earlier sub-scale VCI studies, the heat loss versus time during this 16-minute period was estimated and is shown in Figure 6. A total of 252 Wh of heat energy is lost in the first 16 minutes after hydride deactivation. Although this is roughly ten times the energy lost at the steady-state minimum goal ([100 W][0.27 h] = 27 Wh), the 252 Wh is quite small when compared to the total-battery stored electrical energy (0.6% of 40,000 Wh) or thermal energy (0.8% of 30,000 Wh).

After this transition, the 65 W of minimum enclosure loss plus the 28 W allotted for pass-through loss would result in a battery temperature drop of 0.90 °C/h. Hence, it would take more than 14 hours for the battery temperature to fall from 315°C to 300°C after deactivating the hydride and supplying no additional heat to the batteries (and about 48 hours to fall from 350°C to 300°C).

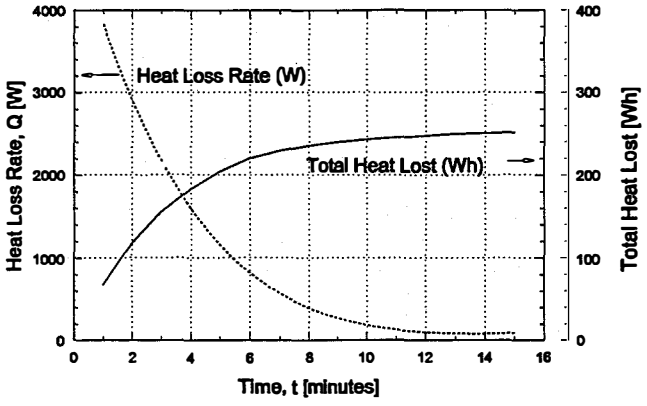

FIGURE 6 - ESTIMATED HEAT LOSS FROM FSTA DURING HYDRIDE DEACTIVATION

CONCLUSIONS

Through sub-scale construction and testing experience and 3-D finite-element structural and thermal analysis, two full-scale test articles were built and tested to demonstrate the feasibility of variable-conductance vacuum insulation as a means of thermal control of high-temperature electric vehicle batteries. The design, which featured multi-component zirconia spacers to separate the thin inner box from the outer vacuum shell, was structurally sound under both pressure and thermal loading. No vibration or shock tests were performed, and sounds heard during severe thermal stressing may indicate that a stronger top spacer or cap may be needed in future designs.

Thermally, the design performed very well. The initial design (FSTA1) had a minimum heat loss 32% greater than the goal (100 W at 300°C). However, improvements were made in the VCI design, and the followup design (FSTA2) lost only 65 W at 300°C (35% less than the goal). The goal of maximum heat removal of 4000 W at 315°C can be obtained at a hydrogen pressure of about 20 torr, and at higher hydrogen pressures, maximum heat removal can be increased to more than 5000 W (at 315°C).

Although small leaks in the welds of the inner box prevented thorough qualification of the hydrides, it appears that hydrogen expulsion and reabsorption rates are adequate for good thermal control. Larger or multiple hydrides will probably be needed to provide the required maximum hydrogen pressure and retain the required hydrogen reabsorption rate over the life of the battery enclosure.

Overall, this work has demonstrated the technical feasibility of the VCI concept for high-temperature batteries. Based on the interest shown by battery manufacturers, future efforts will be directed towards commercialization of the VCI technology.

REFERENCES

Benson, D., Potter, T., and Tracy, C., 1994, "Design of a Variable-Conductance Vacuum Insulation," Soc. of Automotive Engineers Technical Paper 940315.

Burch, S., Potter, T., Keyser, M., Brady, M., and Michaels, K., 1995, "Reducing Cold-Start Emissions by Catalytic Converter Thermal Management," Soc. of Automotive Engineers Technical Paper 941998.

Lee, J., Christianson, C., and Yao, N., 1984, "The Impact of Monoblock Design and Battery Packaging on Temperature Excursion of Nickel/Iron Batteries," Soc. of Automotive Engineers Technical Paper 840473.

Nowbilski, J., and Acharya, A., 1985, "Improved Thermal Insulation for High-Temperature Battery Enclosures," Soc. of Automotive Engineers Technical Paper 859253.

ACKNOWLEDGEMENTS

The authors would like to thank the USABC for sponsorship of this activity, and staff at NREL and Martin Marietta Corporation who assisted in the design and fabrication of the VCI test articles.